On-scalp MEG SQUIDs are sensitive to early somatosensory activity unseen by conventional MEG

NeuroImage 221 (2020) 117157

Contents lists available at ScienceDirect

NeuroImage

journal homepage: www.elsevier.com/locate/neuroimage

On-scalp MEG SQUIDs are sensitive to early somatosensory activity unseen by conventional MEG

Lau M. Andersen [a,b,*], Christoph Pfeiffer [c,d], Silvia Ruffieux [c], Bushra Riaz [e], Dag Winkler [c], Justin F. Schneiderman [e], Daniel Lundqvist [a]

[a] NatMEG, Department of Clinical Neuroscience, Karolinska Institutet, Nobels väg 9, 171 77, Stockholm, Sweden
[b] Center of Functionally Integrative Neuroscience (CFIN), Aarhus University, Nørrebrogade 44, Building 1A, 8000, Aarhus C, Denmark
[c] Department of Microtechnology and Nanoscience – MC2, Chalmers University of Technology, SE-412 96, Gothenburg, Sweden
[d] Department of Neuroscience and Biomedical Engineering, Aalto University School of Science, FI-00076, Aalto, Finland
[e] MedTech West and the Institute of Neuroscience and Physiology, Sahlgrenska Academy, University of Gothenburg, Gothenburg, Sweden

A B S T R A C T

Magnetoencephalography (MEG) has a unique capacity to resolve the spatio-temporal development of brain activity from non-invasive measurements. Conventional MEG, however, relies on sensors that sample from a distance (20–40 mm) to the head due to thermal insulation requirements (the MEG sensors function at 4 K in a helmet). A gain in signal strength and spatial resolution may be achieved if sensors are moved closer to the head. Here, we report a study comparing measurements from a seven-channel on-scalp SQUID MEG system to those from a conventional (in-helmet) SQUID MEG system.

We compared the spatio-temporal resolution between on-scalp and conventional MEG by comparing the discrimination accuracy for neural activity patterns resulting from stimulating five different phalanges of the right hand. Because of proximity and sensor density differences between on-scalp and conventional MEG, we hypothesized that on-scalp MEG would allow for a more high-resolved assessment of these activity patterns, and therefore also a better classification performance in discriminating between neural activations from the different phalanges.

We observed that on-scalp MEG provided better classification performance during an early post-stimulus period (10–20 ms). This corresponded to the electro-encephalographic (EEG) component P16/N16 and was an unexpected observation as this component is usually not observed in conventional MEG. This finding shows that on-scalp MEG enables a richer registration of the cortical signal, indicating a sensitivity to what are potentially sources in the thalamo-cortical radiation.

We had originally expected that on-scalp MEG would provide better classification accuracy based on activity in proximity to the P60m component compared to conventional MEG. This component indeed allowed for the best classification performance for both MEG systems (60–75%, chance 50%). However, we did not find that on-scalp MEG allowed for better classification than conventional MEG at this latency. We suggest that this absence of differences is due to the limited sensor coverage in the recording, in combination with our strategy for positioning the on-scalp MEG sensors. We show how the current sensor coverage may have limited our chances to register the necessary between-phalange source field dissimilarities for fair hypothesis testing, an approach we otherwise believe to be useful for future benchmarking measurements.

1. Introduction

On-scalp magnetoencephalography (MEG) holds great promise for improving MEG in terms of better spatial resolution. In this study, we investigated this promise by comparing the spatial resolution of on-scalp MEG recordings to that of conventional state-of-the-art MEG.

On-scalp MEG technology is becoming increasingly available through the use of high critical temperature (operating at ~77 K) superconducting quantum interference devices (high-T_c SQUIDs (Faley et al., 2013; Öisjöen et al., 2012; Zhang et al., 1993) and optically pumped magnetometers (OPMs) (Boto et al., 2017; Budker and Romalis, 2007). The present on-scalp SQUID sensor technology, though, has significantly higher noise levels than the state-of-the-art MEG sensors, which are operated at 4 K due to their low critical temperature (low-T_c). Hence, while low-T_c SQUIDs (hereafter called in-helmet sensors) demonstrate noise levels of ~3 fT/$\sqrt{\text{Hz}}$, the very best high-T_c sensors show noise levels of ~10 fT/$\sqrt{\text{Hz}}$ (Faley et al., 2006) and often near 50 fT/$\sqrt{\text{Hz}}$ (Pfeiffer et al., 2020b). These differences in noise levels mean that a trade-off might be expected between on-scalp and in-helmet sensors, with on-scalp sensors promising the highest gain in signal-to-noise ratio (SNR) for superficial sources (Iivanainen et al., 2017; Riaz et al., 2017).

A fundamental component of neuroscience research is to elucidate the functional organization of the brain by resolving and discriminating patters of brain activity. EEG has historically played - and plays - a pivotal

* Corresponding author. NatMEG, Department of Clinical Neuroscience, Karolinska Institutet, Nobels väg 9, 171 77, Stockholm, Sweden.
E-mail address: lmandersen@cfin.au.dk (L.M. Andersen).

https://doi.org/10.1016/j.neuroimage.2020.117157
Received 4 June 2020; Accepted 7 July 2020
Available online 11 July 2020

part in revealing especially the temporal properties of these activations. The capacity to spatio-temporally resolve such responses, however, improved markedly with the advent of MEG (Hari et al., 1984; Tiihonen et al., 1989), offering a temporal resolution of <1 ms, and spatial resolution on the millimetre level. In practice however, the spatial resolution depends on a multitude of factors, such as the nature and location of the sources underlying an activity pattern, the distance between the sources and the sensors, the source strength, etc. (Hari and Puce, 2017). Conventional state-of-the-art MEG sensor arrays are typically housed inside a fixed-size helmet and located 20–40 mm away from the scalp of subjects due to the thermal insulation needed to keep the sensors at operational temperature (~4 K). Consequently, because the magnetic field magnitude is roughly inversely proportional to the squared distance between a source and a sensor, on-scalp MEG arrays, wherein magnetometers can be positioned within a few millimetres of the scalp surface, hold great promise for registering weak, but shallow, neural sources (Iivanainen et al., 2017).

Another type of source that on-scalp MEG may be sensitive to are sources from some of the white matter fibres. Specifically, the thalamo-cortical radiation (between thalamus and S1) is a potential candidate. Currents within white matter axons can be modelled by quadropoles, which can be seen as two dipoles with opposite polarities. This makes them invisible when recorded from a distance. However, where white matter tracts have a bend the two dipoles will not have exact opposite polarities. Such signals have been measured using EEG, where the main response component is found at latencies of 15–20 ms post-stimulus (Buchner et al., 1995; Gobbelé et al., 1998). Using a combination of MEG and EEG, this component has been localized to the thalamo-cortical radiation (Götz et al., 2014). When MEG measurement is moved onto the scalp, this also changes the requirements and possibilities for the size of the pick-up coils of magnetometers. Specifically, in order to gain in spatial resolution with on-scalp MEG, high spatial sampling of the neuromagnetic field may be required. The most practical way to achieve this is to reduce the size of the on-scalp pick-up coils, despite a trade-off in terms of increased sensor noise when making pick-up coils smaller. The smaller pickup coils also means that sensors can be packed more closely together than sensors with bigger pickup coils, such as the in-helmet sensors. The combination of sensor proximity and smaller sensor size means that it should be possible to spatially separate neural activity more finely with on-scalp MEG than in-helmet MEG.

To design a test for ascertaining whether on-scalp MEG provides a finer spatial resolution than in-helmet MEG, we devised a stimulation sequence where five different phalanges with varied between-phalange proximity were stimulated on the same hand. The distal phalange of the little finger, the index finger, and the thumb were chosen alongside the middle and proximal phalanges of the index finger. It has been shown that MEG signals can be separately identified from different finger representations in the sensory homunculus (Baumgartner et al., 1991). There is also evidence of the phalanges being separately represented in the sensory homunculus (Druschky et al., 2002).

Our rationale was thus that, due to differences in somatotopic representation, the three phalanges on the index finger and the thumb would be the hardest to discriminate from one another whereas the little finger should more easily be separated from the rest (Baumgartner et al., 1991; Druschky et al., 2002). Because of the gain in sensitivity to magnetic fields, and because of the higher density of sensors, we expected that on-scalp MEG would have an advantage over conventional MEG in terms of discriminating between the activity patterns of these superficial sources that are all close to one another. Tactile stimulations are known to result in a volley of responses with early (<25 ms) and late (>50 ms) components, each of which has a spatio-temporal trajectory evolving along time-courses on the order of milliseconds, as has been revealed by electroencephalography (EEG) (Tsuji and Murai, 1986; Yamada et al., 1984). We expected the classification scores to be maximal around the P60m since this is the strongest of the primary somatosensory responses. Note that this was not a test devised for detecting the thalamo-cortical radiation.

1.1. Snapshot of results

P60m did indeed allow for the best between-phalange classification performance for both MEG systems (60–75%, pairwise comparison, chance 50%). However, we did not find that on-scalp MEG allowed for better classification than conventional MEG. We provide more details on this in the methods and results sections below.

We furthermore observed that on-scalp MEG provided better classification performance during an early post-stimulus period (10–20 ms). This corresponded to the electroencephalographic (EEG) component P16/N16, which is most likely related to the thalamo-cortical radiation from thalamus to S1.

2. Methods

2.1. Subjects

Four subjects were recruited from the scientific team involved in the recordings (four males; aged 49 y, 39 y, 34y and 30 y). The experiment was approved by the Swedish Ethical Review Authority (DNR: 2018/571-31/1), in agreement with the Declaration of Helsinki.

2.2. Stimuli and procedure

The tactile stimulations were generated by using five inflatable membranes (MEG International Services Ltd., Coquitlam, Canada) fastened to the subject's right hand. The membranes were placed on the distal phalange of the little finger (L1), the distal phalange of the thumb (T1) and the three phalanges of the index finger (distal phalange: I1, middle phalange: I2, proximal phalange: I3) (Fig. 1A). The membranes setup was part of a custom stimulation rig (built by Veikko Jousmäki, Aalto University, Finland), which was controlled by pneumatic valves (model SYJ712M-SMU-01F-Q, SMC Corporation, Tokyo, Japan) using 1 bar of pressurised air.

The experimental paradigm consisted of 5000 stimulations evenly distributed between the five phalanges (1000 stimulations each). The inter-stimulus interval (ISI) was 333 ms. Stimulations were ordered in blocks of 10 where the order of stimulations within a block was pseudo-random such that each stimulation type occurred two times in each of these blocks. There was a break in the stimulation sequence every 1250 trials (four total). At the beginning of the experiment, at each break and at the end of the experiment, the sleepiness level of the subject was assessed using the Karolinska Sleepiness Scale KSS (Åkerstedt and Gillberg, 1990). During the stimulation procedure, subjects were watching a television show of their own choice to keep them at a stable level of wakefulness. Audio was provided via sound tubes (model ADU1c, KAR Oy, Helsinki, Finland) rendering the tactile stimulation inaudible. Subjects were instructed to pay full attention to the show and to pay no attention to the stimulations. The subjects held the stimulated hand under a table such that the hand could not be seen.

The experimental paradigm was run three times on each subject, once using conventional in-helmet MEG (Elekta TRIUX) with 102 magnetometers and 204 planar gradiometers; and two times with a seven channel high-T_c SQUID-based on-scalp MEG system (hereafter referred to as the "on-scalp MEG") sampling from two head positions per subject. During all three recordings, nineteen EEG electrodes in a customized 10-20 montage were used to record electrical potentials. The in-helmet MEG was done as a conventional whole-head recording, both for comparison, but also for guiding placement of the on-scalp MEG system.

To project the likely positions of the magnetic field maximum and minimum onto the subjects' heads, an initial localizer protocol was run in in-helmet MEG, using 1000 stimulations to the upper phalange of the index finger (I1). Equivalent Current Dipoles (ECDs) were then fitted to the P60m component of the responses to these stimulations, for each sample point between 45 ms and 65 ms based on the activity of the 102 magnetometers. The magnetic field pattern generated by the dipole with

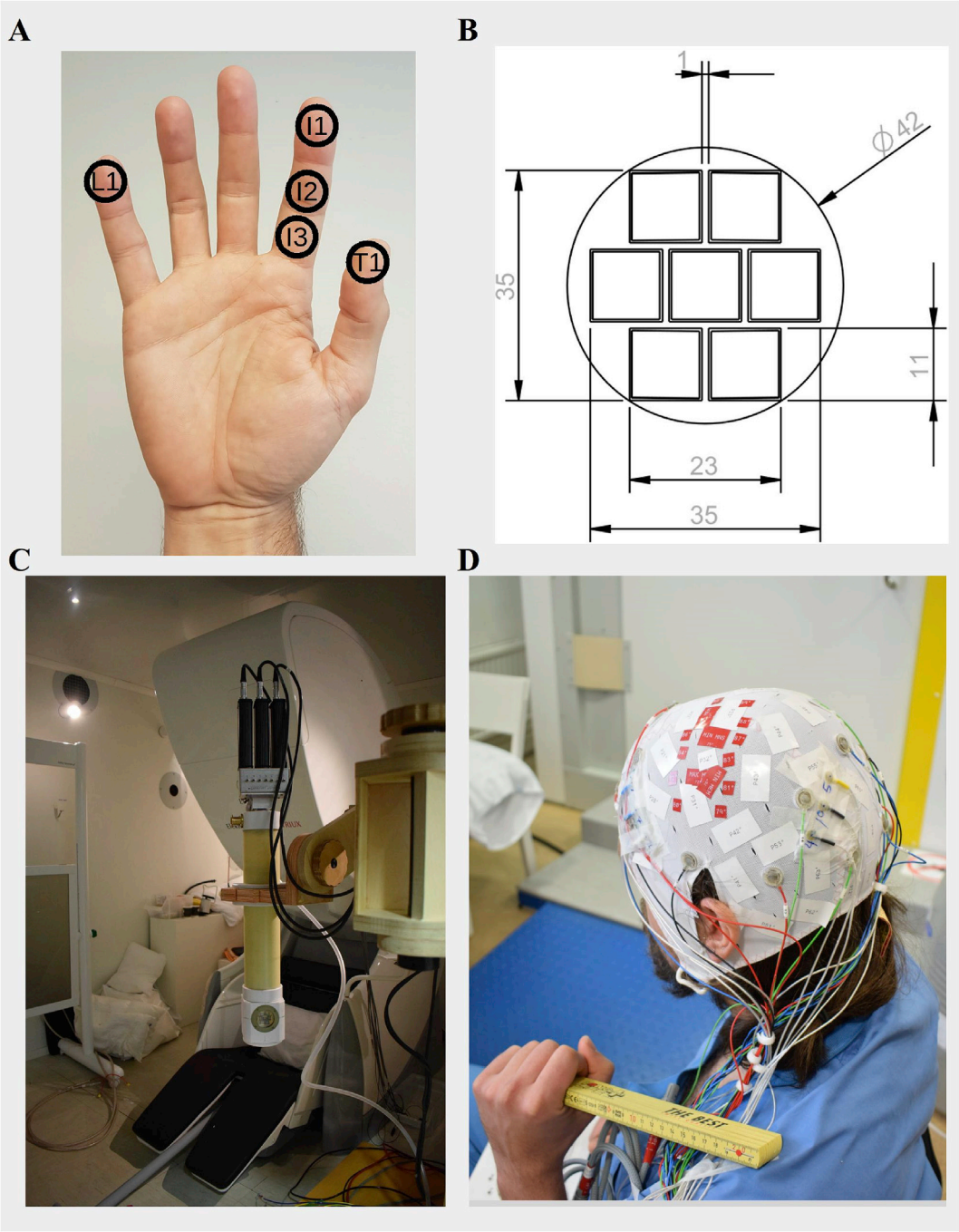

Fig. 1. Illustrations of equipment used. **A:** The five phalanges stimulated **B:** Schematic layout of the sensor array. All measurements are in millimetres. **C:** The on-scalp MEG system cryostat on a wooden articulated armature in front of the in-helmet MEG system. **D:** The customised cap prepared on a subject. The white vinyl markers correspond to the seventy-four channels on the EasyCap 74 channel layout. The larger red vinyl markers indicate the maximum and minimum positions to which the on-scalp MEG was aimed. The smaller red vinyl markers show the fifteen additional coordinate points used to assist and optimize the positioning. Nineteen EEG electrodes were attached in a 10-20 montage (positions Fp1, Fp2, F7, F3, Fz, F4, F8, T7, C3, Cz, C4, T8, P7, P3, Pz, P4, P8, O1 and O2). EEG electrodes that would hinder scalp contact during on-scalp MEG placement were removed at the point of measurement. Nine HPI-coils were placed around the planned recording positions.

the least residual variance was subsequently projected onto the scalp of the subject using a single compartment boundary element method (BEM) volume conduction model based on the subject's anatomy (Gramfort et al., 2013). The centres of the projected maxima and minima were chosen for the recording position of the centre sensor of the on-scalp MEG system (i.e., the centre of the cryostat window over the high-T_c magnetometers). This procedure has been applied successfully before (Andersen et al., 2017; Xie et al., 2016).

2.3. Equipment

All measurements were carried out in a two-layer magnetically shielded room (MSR; model AK3b from Vakuumschmelze GmbH & Co. KG, Hanau, Germany) at the NatMEG facility, Karolinska Institutet, Stockholm, Sweden, http://www.natmeg.se/).

For the in-helmet MEG, an Elekta Neuromag TRIUX (Elekta Oy, Helsinki, Finland) was used. The Elekta Neuromag TRIUX contains 102 sensor chips, each with a magnetometer channel with a pickup loop size

of 21 mm × 21 mm and two orthogonal planar gradiometer channels.

The seven-channel on-scalp MEG-system was made at Chalmers University of Technology (Pfeiffer et al., 2020b). It contains seven high-T_c SQUID magnetometers, each with a pick-up loop size of 9.2 mm × 8.7 mm arranged in a hexagonal array (Fig. 1B). The seven sensors were mounted on a sapphire window connected to a liquid nitrogen vessel inside a vacuum cryostat, the tail of which has a 0.4 mm thick polymer vacuum tight window in front of the sensors. The cryostat is placed on the subject's head with the help of a wooden articulated armature (Fig. 1C). The separation between the scalp and the sensors is about 3 mm or less. The output of the SQUID electronics was recorded using the analogue miscellaneous (MISC) channels of the Elekta TRIUX system, which allowed for sampling the on-scalp data using the same clock as for the in-helmet data and also for synchronizing on-scalp MEG recordings to the EEG data.

Nineteen EEG scalp electrodes were also used, placed in a standard 10-20 layout on a customizable 128 channel cap (Cap and electrodes from EasyCap, BrainVision LLC, USA).

2.4. Preparation of subjects

In preparation for the localizer procedure and the three experimental runs, each subject was fitted with a customized EEG-cap. For the purpose of visualizing a grid of coordinates on an individual's scalp, a total of 89 positions were marked on the 128 channel cap using vinyl markers, from which the first 74 positions were according to the EasyCap 74 channel layout (BrainVision LLC, USA). 15 extra positions were marked out around the area where we expected the P60m field maxima and minima to occur (see Fig. 1D), which served to increase the density of coordinates and aid the final positioning of the on-scalp MEG system. In addition, nine Head Position Indicator (HPI) coils were placed around the expected positions of the maximum and minimum field positions while leaving room for placement of the on-scalp MEG system in between them.

A Polhemus FASTRAK system was used to digitize these eighty-nine positions. In addition, three fiducial points were digitized (the nasion, and the left and right pre-auricular points) as well as the HPI coils. Finally, two-to three-hundred extra head shape points were digitized to aid with co-registration. The reference electrode was placed on the subject's right cheek and the ground electrode on the backside of the neck. For each subject, some of the electrodes had to be removed to leave room for the tail of the cryostat and the HPI-coils. For Subject 1, these were: C3, Cz, P3 and Pz; for Subject 2: C3, Cz and P3; for Subject 3: C3 and Cz; for Subject 4: C3 and Cz.

2.5. Acquisition of data

All data was acquired inside the MSR and was sampled on the Elekta Neuromag TRIUX at a sampling rate of 5000 Hz with an online band-pass filter between 0.1 Hz and 1650 Hz. The nine HPI coils were running continuously at frequencies 1137-1537 Hz with steps of 50 Hz between them. After recording Subject 1, this was changed for the on-scalp recordings, though, because the HPI-coil frequencies were clearly visible on the raw data. For the three subsequent subjects, HPI coils were activated only semi-continuously during regular breaks (30 s) in the on-scalp recordings. Subjects were motivated, comfortably seated with their heads semi-rigidly fixed relative to the on-scalp MEG system, and instructed to be still. It was thus our judgement that running the HPI coils semi-continuously would be sufficient for applying the sensor localization method of Pfeiffer et al. (2018), as also evidenced in Pfeiffer et al. (2019).

2.6. Processing of MEG and EEG data

MNE-Python (Gramfort et al., 2013) was used to read in the raw in-helmet MEG, and on-scalp MEG and EEG data. The raw data was subsequently notch-filtered (50 Hz) and low-pass filtered at 100 Hz, using a one-pass, zero-phase finite impulse response (FIR) filter (order = 78) with a -6dB cutoff frequency of 112.50 Hz. No MaxFiltering was done as it could not be run on the on-scalp recordings. Bad EEG channels, if any, were then marked as bad and the EEG was re-referenced to a common average reference using only the good channels. Subject 1 had no EEG marked as bad; Subject 2 had Fz marked as bad; Subjects 3 and 4 had T8 marked as bad. Among the on-scalp MEG channels, two channels were marked as bad for each subject. For Subject 1: 006 and 007; for Subject 2: 001 and 007; for Subject 3: 001 and 007; for Subject 4: 005 and 007. The filtered data was then segmented into epochs containing data with a 30 ms pre-stimulus period and a 300 ms post-stimulus period. Data was also time-shifted 41 ms to compensate for the delay between the trigger onset and the actual delivery of the pneumatically driven stimulation.

Subsequently, the segmented data was exported to FieldTrip (Oostenveld et al., 2011) where epochs that revealed large variance within them were marked using visually guided tools (Oostenveld et al., 2011). This was done for each on-scalp MEG channel and for each of the in-helmet MEG channels. Finally, event-related fields and potentials (ERFs and ERPs) were calculated from the epochs after having removed those with high variance.

For the in-helmet channels, the peak time was identified for each of the individual phalange P60m components. The two magnetometers with the largest positive and negative response at this time point, respectively, were identified as *the extrema magnetometers*. The six magnetometers geodesically closest to each of the two extrema magnetometers were also identified. These two times seven magnetometers were later to be used in the classification comparisons.

2.7. MR-preprocessing

A full segmentation of earlier acquired T1 MR-images was performed with FreeSurfer (Dale et al., 1999; Fischl et al., 1999). Based on this segmentation the watershed algorithm of FreeSurfer was used to extract surfaces indicating the boundaries for the skin, the skull and the brain. A single compartment volume conductor was subsequently created based on the boundary for the brain surface. For each subject, the T1 was co-registered to the subject's head shape. First, a rough alignment was done using the fiducials. This was subsequently optimized using an Iterative Closest Points algorithm.

2.8. Dipole fits

Finally, a dipole fit was done using MNE-Python for each of the five phalanges based on the in-helmet MEG data. A single dipole was fit based on the data from twenty-six magnetometers at and around the extrema, using gradient descent non-linear optimization for the topographies between 50.0 ms and 70.0 ms in steps of 0.2 ms. We did not fit dipoles for the on-scalp recordings due to the localization procedure not functioning optimally, due to the HPI-frequencies being too close to the online low-pass filter (1650 Hz). (Using lower frequencies the procedure has subsequently been demonstrated to work (Pfeiffer et al., 2020a)). For the EEG, too many electrodes at crucial positions were missing (Fig. 1D).

2.9. Classification of phalanges

For classifications of the phalanges, we used binomial logistic regression (Bishop, 2006). Each phalange was compared pairwise to every other phalange at each time sample. The aim of the classification was to investigate whether the brain's responses would be sufficient to discern which phalange was stimulated. All classifications were performed on sensor-level data within subjects.

For the classification, the 200 trials with the highest variance were removed from the 5000 trials in total. This was done to make the classification models as comparable as possible. Afterwards, for each of the ten possible comparisons, the number of trials for each phalange was equalized. The data was normalized by subtracting the mean and dividing by the variance before being fed to the logistic regression. It was

regularized using the L2 norm, with a regularization value (C) of 1.0. The classifier was trained using cross-validation (ten splits) with a test-train split proportion of 10%/90%. The Python module *Scikit-learn* was used to implement the classification (Pedregosa et al., 2011).

Optimally, all seven on-scalp magnetometers would have been used for the classifications, but for each subject, the on-scalp recording contained two high-noise magnetometers. For the on-scalp data, these comparisons were hence run using only the data of all five low-noise

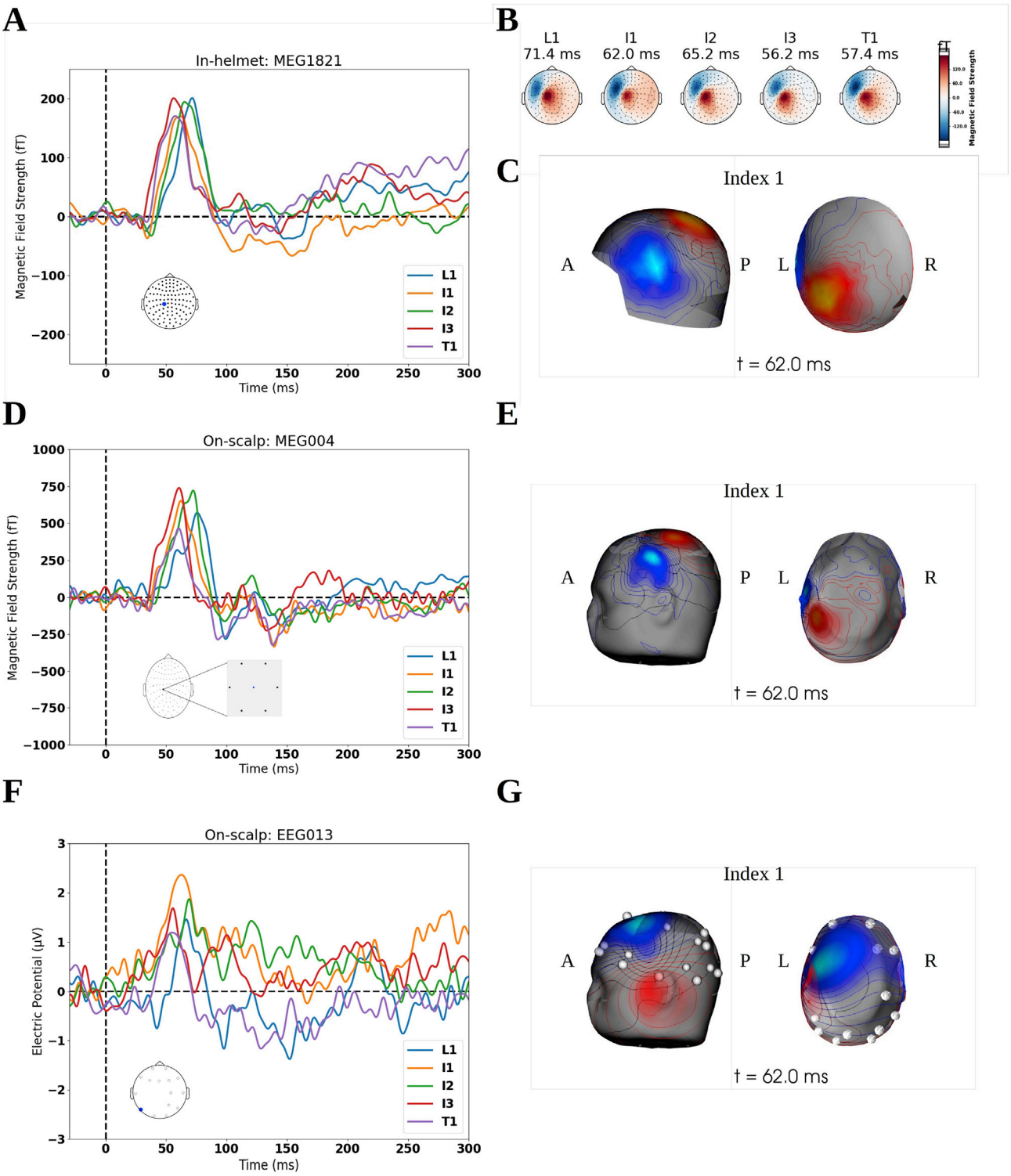

Fig. 2. Summary of activation for Subject 4. **A:** Event-related fields on in-helmet magnetometer reflecting the maximum peaks. **B:** 2d-topographies for the time point where MEG1821 (**A**) has its maximum. **C:** 3d-topography for Index 1 (I1) at its peak. **D:** Event-related fields on on-scalp magnetometer placed on the projected maximum. **E:** The fitted dipole's (Fig. 3) projected magnetic field on the scalp. The blue and red dots are the positions of the centre magnetometer of the cryostat **F:** Event-related potentials on an electrode showing the P60. **G:** The fitted dipole's (Fig. 3) projected electric potential on the scalp. The white dots are the positions of the electrodes. The P60m (panels A and D) and P60 (panel F) are clearly seen for all phalanges though with different peak times.

magnetometers.

To make a fair comparison with the in-helmet data, these comparisons were also run with five in-helmet magnetometers, i.e. the extremum magnetometer and the four geodesically closest neighbours were run. All these analyses were run for the maximum and minimum positions separately.

EEG classification was not run as electrodes around the extrema had to be removed from the setup (Figs. 1D and 2G).

3. Results

In this section, results related to the original hypothesis are presented first, followed by a separate section for the unexpected results related to the early components.

Unless otherwise stated, plots are based on data from Subject 4. This subject is typical in terms of the in-helmet recording and showed some interesting findings in the on-scalp recordings. Plots for all other subjects can be found in the supplementary material.

3.1. Sleepiness scale

No adverse scores on the KSS were reported, showing that subjects were alert and awake.

3.2. Event-related Potentials (ERPs) and Fields (ERFs)

Subjects showed the expected P60m component following the tactile membrane stimulation (Fig. 2). However, within single sensor data, the phalanges differed in their individual P60m peak latencies (Fig. 2ADF; Supplementary Table 1). It can be seen that the peak topographies are very similar, especially within the three phalanges of the index finger. Notably, amplitudes differ more for the on-scalp compared to the in-helmet recordings though. This is likely because the on-scalp sensors sample a smaller area than the in-helmet sensors and/or that closer proximity results in sources changing faster spatially. For the other two fingers, the dipolar fields are slightly rotated relative to the ones for the index finger (Fig. 2B).

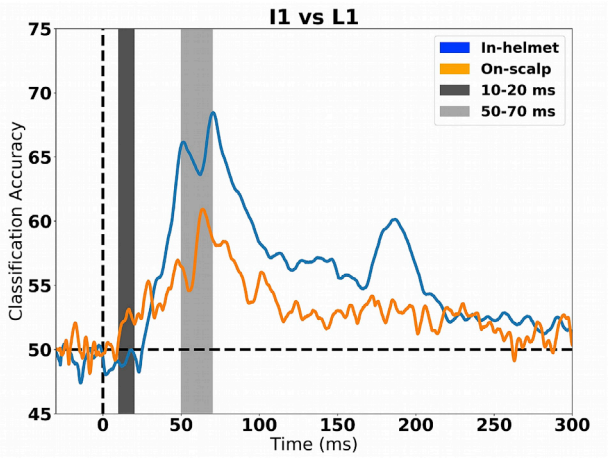

Fig. 4. I1 vs L1 for the maximum position. The peak classification occurred around 50–70 ms (light grey) corresponding to the P60m. An unexpected observation was that the on-scalp classification rises earlier than the in-helmet classification. The 200 trials with the highest variance were removed before classification. See also Supplementary Figs. 4-5.

3.3. Dipole fits

Using the dipole fitting procedure, the P60m components for each phalange were fitted to the primary somatosensory cortex (S1) with mean goodness of fit over all five phalanges being above 90% for all subjects (Fig. 3A). The greatest differences in dipole positions and dipole orientations were found between L1 (little finger, outermost phalange) and the other phalanges, as expected from the somatotopic distance (Fig. 3B). See Supplementary Fig.1 for all subjects.

3.4. Classification – P60m (original hypothesis)

When plotting the peak classification accuracy in the window between 50 ms and 70 ms, the P60m, we found contrary to our hypothesis that in-helmet MEG performed better than on-scalp MEG.

Unexpectedly, we found indications of classification accuracy rising

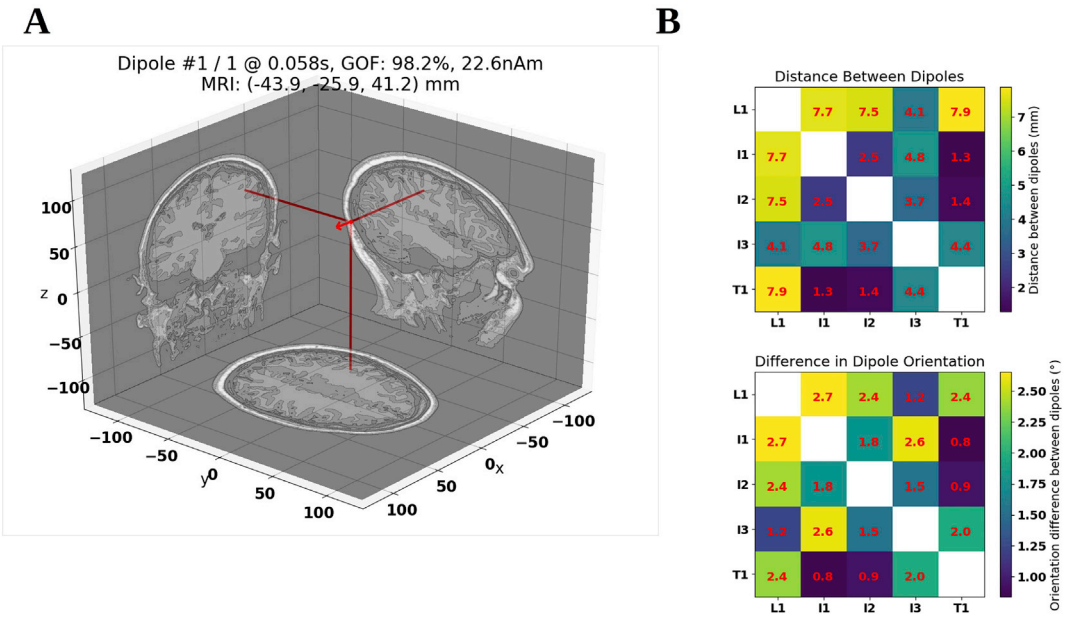

Fig. 3. Dipole fit and peak classifications for Subject 4: **A:** Position and orientation of fitted dipole of I1. The dipole was fitted to contralateral SI. **B:** Distances and orientation differences between fitted dipoles. L1 is the one furthest away from all other dipoles and it also shows the greatest orientation difference compared to the others.

more quickly for the on-scalp MEG as early as from 15 ms (Fig. 4; Supplementary Figs. 4-5).

3.5. Classification – early activity (unexpected results)

To better understand the differences in early classification accuracy, we investigated the early part of the ERFs (Fig. 5). In the maximum recording, we found, visually, that the ERF picked up by one of the on-scalp magnetometers for I1 differed clearly from the others in the time range of 10 ms–20 ms. In the EEG, we found ERPs in this very time range (Fig. 5) (Tsuji and Murai, 1986; Yamada et al., 1984).

3.6. Exploratory testing of early responses

We performed further statistical tests of the early responses in order to assess the influence of Phalanges, Sensors, and their interactions on the signals we detect with the on-scalp and in-helmet systems. Due to the low number of subjects, we decided to do single-subject statistics and estimated the average response in the time window of 10–20 ms for each sensor for each subject. Specifically, we built linear models for each type of recording (on-scalp and in-helmet) where we estimated the average responses in the 10–20 ms time window modelled by the main effects of Phalange (5 levels: L1, I1, I2, I3, T1) and Sensor (On-scalp: 5 levels; In-helmet 7 levels), and the interaction between Phalange and Sensor (reflecting the average response for each Phalange-Sensor pair). These models were built separately from the maximum and minimum recordings. To detect whether or not a given sensor had detected a response in the 10–20 ms interval, a null hypothesis test was done on all phalange/sensor pairs (comparing if the response was significantly different from zero based on a *t*-test; $\alpha = 0.05$). Bonferroni corrections were performed

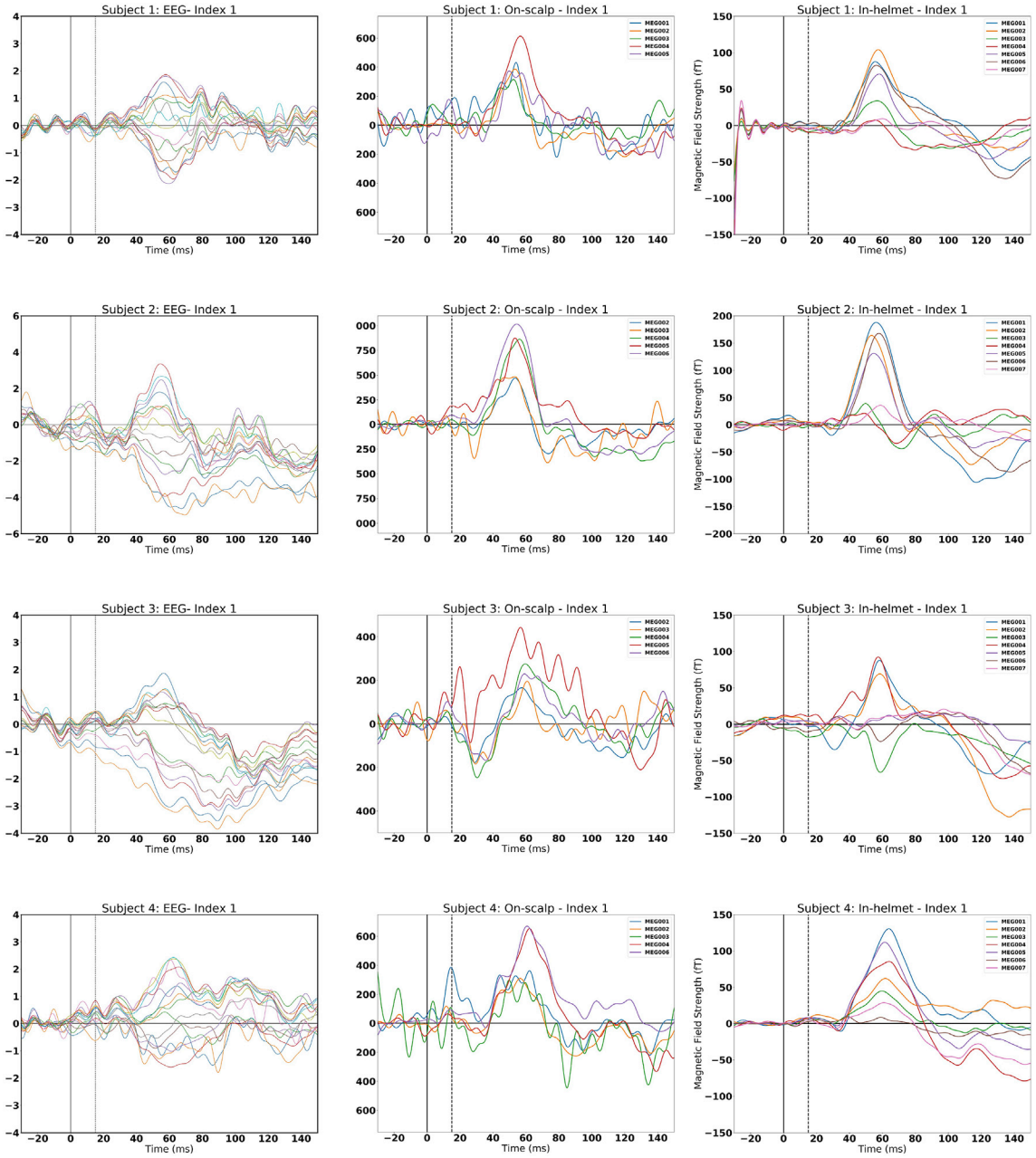

Fig. 5. Evoked responses for Index 1 for all subjects and all sensors. Left column is EEG, middle column is on-scalp and right column is in-helmet. Punctured line for all plots is at 15 ms. All subjects have at least one magnetometer showing a peak at 15 ms for the on-scalp recordings, whereas there are no clear peaks for the in-helmet recordings. See Supplementary Fig. 8 for the minimum recordings. A high-pass filter of 1 Hz has been applied to the EEG recordings.

as this was an exploratory analysis. For all subjects, at least one phalange/sensor pair showed a significant response (after Bonferroni correction) (Table 1) in the on-scalp recordings (Fig. 5). Only one subject had a phalange/sensor pair showing a significant response in the in-helmet recordings.

3.7. Causal filter analysis

A caveat of applying a zero-phase filter is that artificial responses may be created by later responses being pushed forward in time (seemingly occurring earlier than in reality). To investigate whether this was the case for the early response, we did a causal filter analysis (lowpass: 100 Hz), which resulted in the response being pushed 3–4 ms back in time (seemingly occurring later than in reality). The early component was still visible, suggesting that it is not an artefact arising from the zero-phase filter (Supplementary Figs. 2-3 & 6-7).

4. Discussion

In this study, we aimed at comparing the spatio-temporal resolution between on-scalp and in-helmet MEG by assessing the discrimination accuracy for activity patterns resulting from tactile stimulation of five different phalanges of the right hand. Because of differences in sensor-to-cortex proximity as well as in spatial resolution between on-scalp and in-helmet MEG, we hypothesized that on-scalp MEG would allow for better between-phalange classification performance as compared to state-of-the-art MEG.

Our results show that the P60m response component in both on-scalp MEG and in-helmet MEG could be used to successfully discriminate between all the activations patterns of the somatosensory cortex, both between fingers (I1, L1 and T1), and within fingers, across phalanges (I1-I3) (Figs. 3–4, Supplementary Figs. 4-5). However, our initial hypothesis that on-scalp MEG would allow for better classification performance as compared to state-of-the-art MEG around the P60m was not confirmed. If anything, it was the other way around with in-helmet magnetometers outperforming on-scalp magnetometers. We discuss the possible reasons to and implications of this in a separate section below ("Further discussion of P60m classification").

4.1. Early activity (10–20 ms)

The comparison of on-scalp and in-helmet discrimination accuracy however also generated an incidental finding, where on-scalp MEG recordings resulted in a superior classification performance as compared to in-helmet MEG. These findings stem from the time period *before* the rise of the P60m, in the time range of 10–20 ms (Figs. 4–5) and were linked to the P16/N16 component found in EEG recordings (Fig. 5). Furthermore, these responses were seen only in the on-scalp MEG and not in the in-helmet MEG data (Fig. 5).

4.2. Thalamo-cortical radiation

In all our subjects, we observed an early response component, peaking around 16 ms (Fig. 5 & Supplementary Figs. 4-5). Several EEG studies have provided evidence that the thalamo-cortical radiation between thalamus and S1 can be picked up around this time (Buchner et al., 1995; Gobbelé et al., 2004; Götz et al., 2014). It might also be possible to measure this response with MEG, even though that is considered to be complicated by these sources being deep and extending towards the centre of the brain. For example, the recent study of Antonakakis et al. (2019) did not report evidence of the N16/P16 component when investigating the N20/P20. Some evidence has been found of the thalamo-cortical radiation being possible to reconstruct with dipole fitting using conventional MEG (Kimura et al., 2008; Papadelis et al., 2012). These studies however did not find a clear response component in the sensor-level data, such as we did in our on-scalp MEG measurement (but did not in our in-helmet measurement), but based their source reconstruction on *a priori* information from functional Magnetic Resonance Imaging (fMRI) and EEG studies.

Table 1
Single-subject statistics for the average amplitude based on the linear models described above. Only tests that are significant at $\alpha = 0.05$ when Bonferroni corrected are shown. All on-scalp recordings show at least one response that is significantly different from zero, whereas only Subject 3 has significant responses for the in-helmet recordings. The number of tests was 35 for in-helmet recordings and 25 for on-scalp recordings. See Supplementary Table (1) for the full table.

Subject	Type	Sign	Phalange-sensor pair	*p* (uncorrected)	*p* (Bonferroni-corrected)
1	On-scalp	+	I1 MEG001	0.0011	0.028
1	On-scalp	–	I2 MEG001	<0.001	<0.001
2	On-scalp	+	I1 MEG005	<0.001	0.022
3	On-scalp	+	I1 MEG005	<0.001	<0.001
3	On-scalp	+	I2 MEG005	<0.001	0.0014
3	On-scalp	–	I1 MEG005	<0.001	0.013
3	In-helmet	–	T1 MEG002	<0.001	0.0050
3	In-helmet	–	T1 MEG004	<0.001	0.033
3	In-helmet	–	T1 MEG006	0.0010	0.035
4	On-scalp	+	I1 MEG001	<0.001	<0.001
4	On-scalp	+	T1 MEG003	0.0019	0.047
4	On-scalp	–	I3 MEG003	<0.001	0.0027
4	On-scalp	–	T1 MEG001	<0.001	<0.001
4	On-scalp	–	T1 MEG004	<0.001	<0.001

4.3. Further discussion of P60m classification

The motivation for the hypothesis that on-scalp classification would result in better classification than in-helmet classification was the improved sensor-to-brain proximity, combined with the associated gain in SNR, and the increased sensor density. A feature of the data that we could not fully evaluate beforehand here is whether the sensor array would be large enough to pick up both the common activations between phalanges *and* the unique activations for each phalange. To investigate whether this factor was involved in shaping the results in our study, we evaluated the overlap of activations for each phalange at 60 ms (Fig. 6). See Supplementary Fig. 9 for all subjects.

These plots of overlapping fields indicated that the on-scalp MEG sensor array mostly picked up signal from areas that overlap either completely or greatly in terms of signal strength (Fig. 6A). For the in-helmet MEG sensors used, results show less overlap between sensors (Fig. 6B). Consequently, it was the case that the signal at each measurement point was more homogeneous within the area covered by the on-scalp MEG than by the in-helmet MEG sensors indicating that we had placed the on-scalp MEG at sub-optimal positions.

4.4. Future directions

The findings above indicate that to fully evaluate our initial hypothesis regarding the spatio-temporal resolution from on-scalp and in-helmet measurements for the P60m, it would be necessary to repeat this study with an on-scalp sensor array that covers both field commonalities and field differences for the involved between-phalange

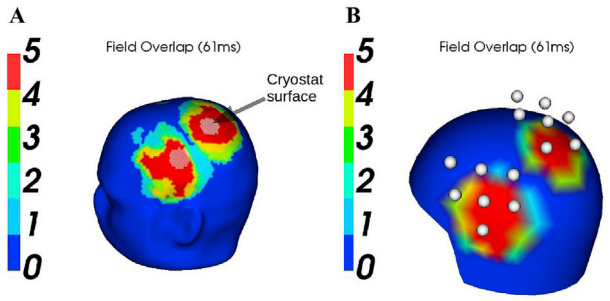

Fig. 6. Relation between spread of field and sensor positions for Subject 4. **A:** The overlap of fields generated by the dipole models for each phalange at 61 ms is illustrated. The lower and upper fifth percentiles of magnetic field strength on the head were calculated for each of these dipole models. The colour map indicates where these percentiles overlap. The white dots indicate the surface of the cryostat. It is seen that the cryostat was placed where the fields overlap either completely or at least four out of five do. **B:** The same plot for the in-helmet recording, but the white dots indicate the actual positions of the seven sensors used for classification. Note that the overlap between the fields here is visibly different from the **A** panel. Note also that these figures were created with dipole fits based on data that had been lowpass filtered at 30 Hz. See also Supplementary Fig. 9.

comparisons; or in the absence of a larger sensor array at least record positions around the extrema to provide full coverage of the fields.

It would also be of great interest to further explore the early activity measured here likely P16m, more thoroughly, using a more direct and dedicated paradigm. A suggested route forward would be to first localize the P16/N16 component, preferably using high-density EEG. Then, the corresponding MEG field could be projected using anatomically accurate volume conductors. The on-scalp sensors could then be placed optimally in accordance with these projections. Another option, which is possible with extensive on-scalp MEG sensor coverage, such as already possible with OPMs, the whole somatosensory cortex (and beyond) may be covered at one go. One could of course also use a small sensor array as here but perform recordings at several places above the somatosensory cortex so to accumulate coverage of a larger area.

5. Conclusions

In our comparison of spatio-temporal resolution between on-scalp and in-helmet MEG, we did not find the initially hypothesized improved spatial discrimination for on-scalp MEG compared to in-helmet MEG around the P60m. We suggest that an important reason for this unexpected finding is that the fields associated with the five phalanges overlap to a high degree, and that the on-scalp sensors covered too small an area to fully discern the differences between these fields (Fig. 6).

In an unexpected finding, we show that the on-scalp MEG classified the phalanges better than the in-helmet MEG during an early time period (10–20 ms), which may reflect the P16m component. We propose that these findings stem from the improved signal gain and/or the increase in spatial sensor resolution using on-scalp MEG.

Acknowledgements

This work was funded by the Knut and Alice Wallenberg Foundation (KAW2014.0102), the Swedish Research Council (2017-00680), and the Swedish Childhood Cancer Foundation (MT2018-0020). Data for this study was collected at NatMEG, the National Facility for Magnetoencephalography, Karolinska Institutet, Sweden. The NatMEG facility is supported by Knut & Alice Wallenberg (KAW2011.0207). We also acknowledge the contribution of Veikko Jousmäki, Aalto University, Finland for building the custom stimulation system.

Appendix A. Supplementary data

Supplementary data to this article can be found online at https://doi.org/10.1016/j.neuroimage.2020.117157.

References

Åkerstedt, T., Gillberg, M., 1990. Subjective and objective sleepiness in the active individual. Int. J. Neurosci. 52, 29–37. https://doi.org/10.3109/00207459008994241.

Andersen, L.M., Oostenveld, R., Pfeiffer, C., Ruffieux, S., Jousmäki, V., Hämäläinen, M., Schneiderman, J.F., Lundqvist, D., 2017. Similarities and differences between on-scalp and conventional in-helmet magnetoencephalography recordings. PloS One 12, e0178602. https://doi.org/10.1371/journal.pone.0178602.

Antonakakis, M., Schrader, S., Wollbrink, A., Oostenveld, R., Rampp, S., Haueisen, J., Wolters, C.H., 2019. The effect of stimulation type, head modeling, and combined EEG and MEG on the source reconstruction of the somatosensory P20/N20 component. Hum. Brain Mapp. 40, 5011–5028. https://doi.org/10.1002/hbm.24754.

Baumgartner, C., Doppelbauer, A., Sutherling, W.W., Zeitlhofer, J., Lindinger, G., Lind, C., Deecke, L., 1991. Human somatosensory cortical finger representation as studied by combined neuromagnetic and neuroelectric measurements. Neurosci. Lett. 134, 103–108. https://doi.org/10.1016/0304-3940(91)90518-X.

Bishop, C.M., 2006. Pattern Recognition and Machine Learning. Springer, USA, Cambridge, UK.

Boto, E., Meyer, S.S., Shah, V., Alem, O., Knappe, S., Kruger, P., Fromhold, T.M., Lim, M., Glover, P.M., Morris, P.G., Bowtell, R., Barnes, G.R., Brookes, M.J., 2017. A new generation of magnetoencephalography: room temperature measurements using optically-pumped magnetometers. Neuroimage 149, 404–414. https://doi.org/10.1016/j.neuroimage.2017.01.034.

Buchner, H., Waberski, T.D., Fuchs, M., Wischmann, H.-A., Beckmann, R., Rienäcker, A., 1995. Origin of P16 median nerve SEP component identified by dipole source analysis — subthalamic or within the thalamo-cortical radiation? Exp. Brain Res. 104, 511–518. https://doi.org/10.1007/BF00231985.

Budker, D., Romalis, M., 2007. Optical magnetometry. Nat. Phys. 3, 227–234. https://doi.org/10.1038/nphys566.

Dale, A.M., Fischl, B., Sereno, M.I., 1999. Cortical surface-based analysis. I. Segmentation and surface reconstruction. Neuroimage 9, 179–194. https://doi.org/10.1006/nimg.1998.0395.

Druschky, K., Kaltenhäuser, M., Hummel, C., Druschky, A., Pauli, E., Huk, W.J., Stefan, H., Neundörfer, B., 2002. Somatotopic organization of the ventral and dorsal finger surface representations in human primary sensory cortex evaluated by magnetoencephalography. Neuroimage 15, 182–189. https://doi.org/10.1006/nimg.2001.0920.

Faley, M.I., Poppe, U., Dunin-Borkowski, R.E., Schiek, M., Boers, F., Chocholacs, H., Dammers, J., Eich, E., Shah, N.J., Ermakov, A.B., Slobodchikov, V.Y., Maslennikov, Y.V., Koshelets, V.P., 2013. High- DC SQUIDs for magnetoencephalography. IEEE Trans. Appl. Supercond. 23 https://doi.org/10.1109/TASC.2012.2229094, 1600705–1600705.

Faley, M.I., Poppe, U., Urban, K., Paulson, D.N., Fagaly, R.L., 2006. A new generation of the HTS multilayer DC-SQUID magnetometers and gradiometers. J. Phys. Conf. Ser. 43, 1199–1202. https://doi.org/10.1088/1742-6596/43/1/292.

Fischl, B., Sereno, M.I., Dale, A.M., 1999. Cortical surface-based analysis: II: inflation, flattening, and a surface-based coordinate system. Neuroimage 9, 195–207. https://doi.org/10.1006/nimg.1998.0396.

Gobbelé, R., Buchner, H., Curio, G., 1998. High-frequency (600 Hz) SEP activities originating in the subcortical and cortical human somatosensory system. Electroencephalogr. Clin. Neurophysiol. Potentials Sect. 108, 182–189. https://doi.org/10.1016/S0168-5597(97)00100-7.

Gobbelé, R., Waberski, T.D., Simon, H., Peters, E., Klostermann, F., Curio, G., Buchner, H., 2004. Different origins of low- and high-frequency components (600 Hz) of human somatosensory evoked potentials. Clin. Neurophysiol. 115, 927–937. https://doi.org/10.1016/j.clinph.2003.11.009.

Götz, T., Huonker, R., Witte, O.W., Haueisen, J., 2014. Thalamocortical impulse propagation and information transfer in EEG and MEG. J. Clin. Neurophysiol. Off. Publ. Am. Electroencephalogr. Soc. 31, 253–260. https://doi.org/10.1097/WNP.0000000000000048.

Gramfort, a., Luessi, M., Larson, E., Engemann, D., Strohmeier, D., Brodbeck, C., Parkkonen, L., Hämäläinen, M., 2013. MNE software for processing MEG and EEG data. Neuroimage. https://doi.org/10.1016/j.neuroimage.2013.10.027.

Hari, R., Puce, A., 2017. MEG-EEG Primer. Oxford University Press, New York, NY, US.

Hari, R., Reinikainen, K., Kaukoranta, E., Hämäläinen, M., Ilmoniemi, R., Penttinen, A., Salminen, J., Teszner, D., 1984. Somatosensory evoked cerebral magnetic fields from SI and SII in man. Electroencephalogr. Clin. Neurophysiol. 57, 254–263. https://doi.org/10.1016/0013-4694(84)90126-3.

Iivanainen, J., Stenroos, M., Parkkonen, L., 2017. Measuring MEG closer to the brain: performance of on-scalp sensor arrays. Neuroimage 147, 542–553. https://doi.org/10.1016/j.neuroimage.2016.12.048.

Kimura, T., Ozaki, I., Hashimoto, I., 2008. Impulse propagation along thalamocortical fibers can Be detected magnetically outside the human brain. J. Neurosci. 28, 12535–12538. https://doi.org/10.1523/JNEUROSCI.3022-08.2008.

Öisjöen, F., Schneiderman, J.F., Figueras, G.A., Chukharkin, M.L., Kalabukhov, A., Hedström, A., Elam, M., Winkler, D., 2012. High-Tc superconducting quantum interference device recordings of spontaneous brain activity: towards high-Tc

magnetoencephalography. Appl. Phys. Lett. 100, 132601 https://doi.org/10.1063/1.3698152.

Oostenveld, R., Fries, P., Maris, E., Schoffelen, J.-M., 2011. FieldTrip: open source software for advanced analysis of MEG, EEG, and invasive electrophysiological data. Comput. Intell. Neurosci., 156869 https://doi.org/10.1155/2011/156869, 2011.

Papadelis, C., Leonardelli, E., Staudt, M., Braun, C., 2012. Can magnetoencephalography track the afferent information flow along white matter thalamo-cortical fibers? Neuroimage 60, 1092–1105. https://doi.org/10.1016/j.neuroimage.2012.01.054.

Pedregosa, F., Varoquaux, G., Gramfort, A., Michel, V., Thirion, B., Grisel, O., Blondel, M., Prettenhofer, P., Weiss, R., Dubourg, V., Vanderplas, J., Passos, A., Cournapeau, D., Brucher, M., Perrot, M., Duchesnay, É., 2011. Scikit-learn: machine learning in Python. J. Mach. Learn. Res. 12, 2825–2830.

Pfeiffer, C., 2019. On-scalp MEG Using High-Tc SQUIDs: Measuring Brain Activity with Superconducting Magnetometers. Chalmers University of Technology.

Pfeiffer, C., Andersen, L.M., Lundqvist, D., Hämäläinen, M., Schneiderman, J.F., Oostenveld, R., 2018. Localizing on-scalp MEG sensors using an array of magnetic dipole coils. PloS One 13, e0191111. https://doi.org/10.1371/journal.pone.0191111.

Pfeiffer, C., Ruffieux, S., Andersen, L.M., Kalabukhov, A., Winkler, D., Oostenveld, R., Lundqvist, D., Schneiderman, J.F., 2020. On-scalp MEG sensor localization using magnetic dipole-like coils: a method for highly accurate co-registration. Neuroimage 212, 116686. https://doi.org/10.1016/j.neuroimage.2020.116686.

Pfeiffer, C., Ruffieux, S., Jönsson, L., Chukharkin, M.L., Kalaboukhov, A., Xie, M., Winkler, D., Schneiderman, J.F., 2020. A 7-channel high-Tc SQUID-based on-scalp MEG system. IEEE Trans. Biomed. Eng. 67, 1483–1489. https://doi.org/10.1109/TBME.2019.2938688.

Riaz, B., Pfeiffer, C., Schneiderman, J.F., 2017. Evaluation of realistic layouts for next generation on-scalp MEG: spatial information density maps. Sci. Rep. 7, 6974. https://doi.org/10.1038/s41598-017-07046-6.

Tiihonen, J., Hari, R., Hämäläinen, M., 1989. Early deflections of cerebral magnetic responses to median nerve stimulation. Electroencephalogr. Clin. Neurophysiol. Potentials Sect. 74, 290–296. https://doi.org/10.1016/0168-5597(89)90059-2.

Tsuji, S., Murai, Y., 1986. Scalp topography and distribution of cortical somatosensory evoked potentials to median nerve stimulation. Electroencephalogr. Clin. Neurophysiol. Potentials Sect. 65, 429–439. https://doi.org/10.1016/0168-5597(86)90022-5.

Xie, M., Schneiderman, J., Chukharkin, M., Kalabukhov, A., Riaz, B., Lundqvist, D., Whitmarsh, S., Hamalainen, M., Jousmaki, V., Oostenveld, R., Winkler, D., 2016. Benchmarking for on-scalp MEG sensors. IEEE Trans. Biomed. Eng. https://doi.org/10.1109/TBME.2016.2599177, 1–1.

Yamada, T., Kayamori, R., Kimura, J., Beck, D.O., 1984. Topography of somatosensory evoked potentials after stimulation of the median nerve. Electroencephalogr. Clin. Neurophysiol. Potentials Sect. 59, 29–43. https://doi.org/10.1016/0168-5597(84)90018-2.

Zhang, Y., Tavrin, Y., Mück, M., Braginski, A.I., Heiden, C., Hampson, S., Pantev, C., Elbert, T., 1993. Magnetoencephalography using high temperature rf SQUIDs. Brain Topogr. 5, 379–382. https://doi.org/10.1007/BF01128694.